ADVANCED ENGINEERING MATERIALS

DOI: 10.1002/adem.201100080

Influence of Pressing Temperature on Microstructure Evolution and Mechanical Behavior of Ultrafine-Grained Cu Processed by Equal-Channel Angular Pressing**

By *Haiming Wen,* Yonghao Zhao, Troy D. Topping, Dustin Ashford, Roberto B. Figueiredo, Cheng Xu, Terence G. Langdon* and *Enrique J. Lavernia*

Pure Cu was processed by ECAP at five different temperatures from room temperature (RT) to 523 K. The influence of pressing temperature on microstructure evolution and tensile behavior was investigated in detail. The results show that as the ECAP temperature is increased the grain size and ductility both increase whereas the dislocation density and yield strength decrease. In the case of ECAP processing in the range of RT to 473 K the mechanism governing microstructural refinement is continuous dynamic recrystallization (CDRX), whereas at 523 K the mechanism changes to discontinuous dynamic recrystallization (DDRX). At higher ECAP temperatures, the kinetics of CDRX are retarded leading to a lower fraction of equiaxed grains/high-angle grain boundaries and a higher fraction of dislocation cell structures. At 523 K, DDRX induces a high fraction of equiaxed grains with a very low dislocation density which appears responsible for the observed high tensile ductility. The sample processed at 523 K possessed a good combination of strength and ductility, suggesting that processing by ECAP at elevated temperatures may be a suitable alternative to RT ECAP processing followed by subsequent annealing.

[*] *H. M. Wen, Dr. Y. H. Zhao, T. D. Topping, D. Ashford, Prof. E. J. Lavernia*
Department of Chemical Engineering and Materials Science, University of California at Davis, Davis, CA 95616, (USA)
E-mail: hmwen@ucdavis.edu
Dr. R. B. Figueiredo
Department of Metallurgical and Materials Engineering, Universidade Federal de Minas Gerais, Belo Horizonte, Minas Gerais 31270-901, (Brazil)
Prof. C. Xu
Ningbo Institute of Materials Technology and Engineering, Chinese Academy of Sciences, Ningbo, Zhejiang 315201, (PR China)
Prof. T. G. Langdon
Departments of Aerospace and Mechanical Engineering and Materials Science, University of Southern California, Los Angeles, CA 90089-1453, (USA)
Materials Research Group, School of Engineering Sciences, University of Southampton, Southampton SO17 1BJ, (UK)

[**] *Financial support from the Office of Naval Research (N00014-08-1-0405) is gratefully acknowledged. Research at the University of Southern California was supported by the National Science Foundation of the United States under Grant No. DMR-0855009.*

Equal-channel angular pressing (ECAP), as a technique of severe plastic deformation (SPD), has been widely used to produce ultrafine-grained (UFG) structures in metallic materials.[1] Inspection of the published literature shows that the relevant ECAP processing parameters, such as the processing route,[2–5] channel angle,[6,7] angle of curvature,[8] cumulative strain,[3,9] pressing speed,[9] and pressing temperature,[10,11] influence the ultimate microstructure obtained. However, it is worth noting that amongst these various parameters the influence of pressing temperature has been studied the least.

Elevated temperature ECAP provides some inherent benefits. For example, pressing can be more readily conducted at higher temperatures because of the lower pressures required since the strength of the material to be pressed decreases with temperature. In addition, an increased pressing temperature normally leads to improvements in plastic workability, which is especially beneficial for samples with limited ductility.[12,13] Processing by ECAP at elevated temperatures has been applied to introduce grain refinement in relatively brittle metals and alloys.[14–19]

The effect of pressing temperature on microstructural development during ECAP represents an important area of study and it has been investigated by some researchers,

mostly on Al and Al alloys, with the general conclusion that a higher pressing temperature leads to a larger grain size and a higher fraction of low-angle boundaries.[10–13,20–25] However, the effect of pressing temperature on the mechanical behavior of the materials processed by ECAP has not been systematically examined. In addition, ECAP at elevated temperatures has been rarely reported for the processing of Cu[26] although ECAP of Cu at room temperature (RT)[27–34] has been reported extensively. This is surprising since Cu represents an ideal model material for studies of microstructure evolution and mechanical behavior due to its fcc crystal structure, medium stacking fault energy and good formability. The microstructural refinement processes/mechanisms in Cu during ECAP at elevated temperatures remain poorly understood and it is likely that they differ from those in Al and Al alloys since Cu has a significantly lower stacking fault energy.

The UFG materials produced by SPD generally have poor ductility because of a very low strain hardening rate which is ascribed both to the small grain size and the consequent limited space for dislocation storage and to the high initial dislocation density and the rapid saturation of dislocations during subsequent deformation.[35] Annealing, which reduces the dislocation density and increases the grain size, is regularly conducted after SPD to improve the ductility of the SPD-processed UFG materials.[36,37] Therefore, ECAP at RT followed by annealing at higher temperatures is widely applied to achieve a balanced strength and ductility. The application of higher ECAP temperatures may simplify the processes by eliminating the need for an annealing treatment. Moreover, it is generally easier, from an experimental standpoint, to press specimens at higher temperatures than at RT. However, a comparison is needed between the mechanical behavior achieved by ECAP at elevated temperatures and that obtained by ECAP at RT followed by annealing at higher temperatures.

In view of the above discussion, the present study was undertaken with three primary objectives. First, to investigate the influence of the ECAP temperature on the microstructural refinement and the mechanical behavior of Cu. Second, to evaluate the feasibility of using elevated-temperature ECAP as an approach to avoid the need for an annealing step following RT ECAP in an effort to obtain good combinations of strength and ductility. Third, to provide fundamental insight into the mechanisms that govern microstructural evolution and mechanical behavior of Cu processed by elevated temperature ECAP. To accomplish these objectives, ECAP was conducted on coarse-grained Cu at five different temperatures from RT to 523 K, and the microstructural evolution during ECAP and mechanical behavior of the ECAP-processed samples were examined using transmission electron microscopy (TEM) and tensile testing.

1. Experimental

The starting materials were coarse-grained pure Cu rods (purity 99.9%, with 0.030% Ni, 0.025% Te, 0.018% Sb, 0.013% As, 0.004% O, and Ag, Bi, P, Mg, Si, Sn, Fe, Pb all <0.002%) with a diameter of 10 mm, and the ECAP die was circular with the same diameter. The ECAP die had L-shaped channels with an angle of 90° between the two channels and an angle at the outer arc of 20° which imposed an effective strain of approximately one per ECAP pass.[38] Five different processing temperatures were used: RT, 373, 423, 473, and 523 K. For ECAP at elevated temperatures, the die was heated using horizontal heating plates and then maintained at the required pressing temperature to within ±5 K. The billet was inserted into the entrance channel of the die and remained in the channel for about 5 min to reach the required temperature. During pressing, the plunger speed was about $7\,mm \cdot s^{-1}$. Samples were processed for eight passes except at RT where they were pressed through three passes, and all pressing was conducted using route B_C in which the samples were rotated by 90° in the same sense with respect to the previous pass,[39] since microstructural evolution occurs most rapidly when using route B_C.[4,39] The pressed samples were quenched in water after ECAP.

Flat dog-bone tensile specimens with gauge dimensions of $10 \times 1 \times 2\,mm^3$ were sectioned by electrical discharge machining (EDM) from the central regions of the Cu rods after ECAP with the gauge axes parallel to the extrusion direction. All tensile specimens were finally polished using a diamond suspension with a particle size of 0.25 μm. Uniaxial tensile tests were performed at RT by an Instron 8801 universal testing machine (UTM) equipped with Bluehill 2 software, using an initial quasi-static strain rate of $1.0 \times 10^{-3}\,s^{-1}$. The strain was measured using a standard non-contacting video extensometer with a 100 mm field-of-view lens. The stress–strain curves were recorded for each specimen, and these curves were used to determine the 0.2% proof strength and uniform elongation. Two tensile specimens were made and therefore two tensile tests were performed for each ECAP-processed sample.

Thin foils for TEM analysis were sectioned from the central part of the cross section (traverse plane normal to the extrusion direction) of the as-pressed rods. The TEM specimens were obtained by mechanically grinding and dimpling the thin foils to a thickness of ≈10 μm, and further thinning to electron transparency using a Gatan PIPS 691 ion milling system. The TEM observations were carried out on a Philips CM12 microscope working at 120 kV and a JEOL 2500SE microscope operating at 200 kV. Selected area electron diffraction (SAED) patterns were recorded using apertures with diameters of ≈6 μm and 100 nm for the CM12 and JEOL 2500SE instruments, respectively.

Grain size measurements were conducted using an Olympus analySIS FIVE software. For each grain size measurement, a contour was drawn along the boundary of the grain, and the software automatically provided the mean diameter of the grain by measuring and averaging 180 diameters for angles in the range 0° through 179° with a step width of 1°. The relative error of this method of grain size measurement is estimated as less than 3%. For each sample,

ADVANCED ENGINEERING MATERIALS

grain size measurements were conducted on grains with clearly defined grain boundaries which were usually nearly equiaxed using 80 TEM images recorded by CM12. The average grain size was obtained from at least 70 up to 500 grains, where in practice the number of grain size measurements depended on the availability of appropriate grains in the 80 TEM images of the sample.

High resolution TEM (HRTEM) images of lattice fringes were taken by JEOL 2500SE, which has a spherical aberration of 1.0 mm and an achievable best point-to-point resolution of 1.4 Å, to determine the dislocation density. For each sample, three grains were imaged in order to obtain the density. Specifically, a grain was tilted to the [011] zone axis and at least 20 lattice-fringe images of the grain were recorded at the same magnification. Inverse Fourier transformation was performed on an HRTEM image to obtain the $(\bar{1}1\bar{1})$ crystallographic planes, and the number of dislocations in the image was counted. The same procedure was carried out for all the ≈60 HRTEM images of a sample, and the dislocation density of the sample was determined by dividing the average number of dislocations per image by the area of an image.

2. Results and Discussion

2.1 Microstructures after ECAP below 523 K

The microstructures of the UFG Cu samples processed by ECAP at different temperatures varied significantly. Figure 1 presents the bright-field TEM images of all five samples

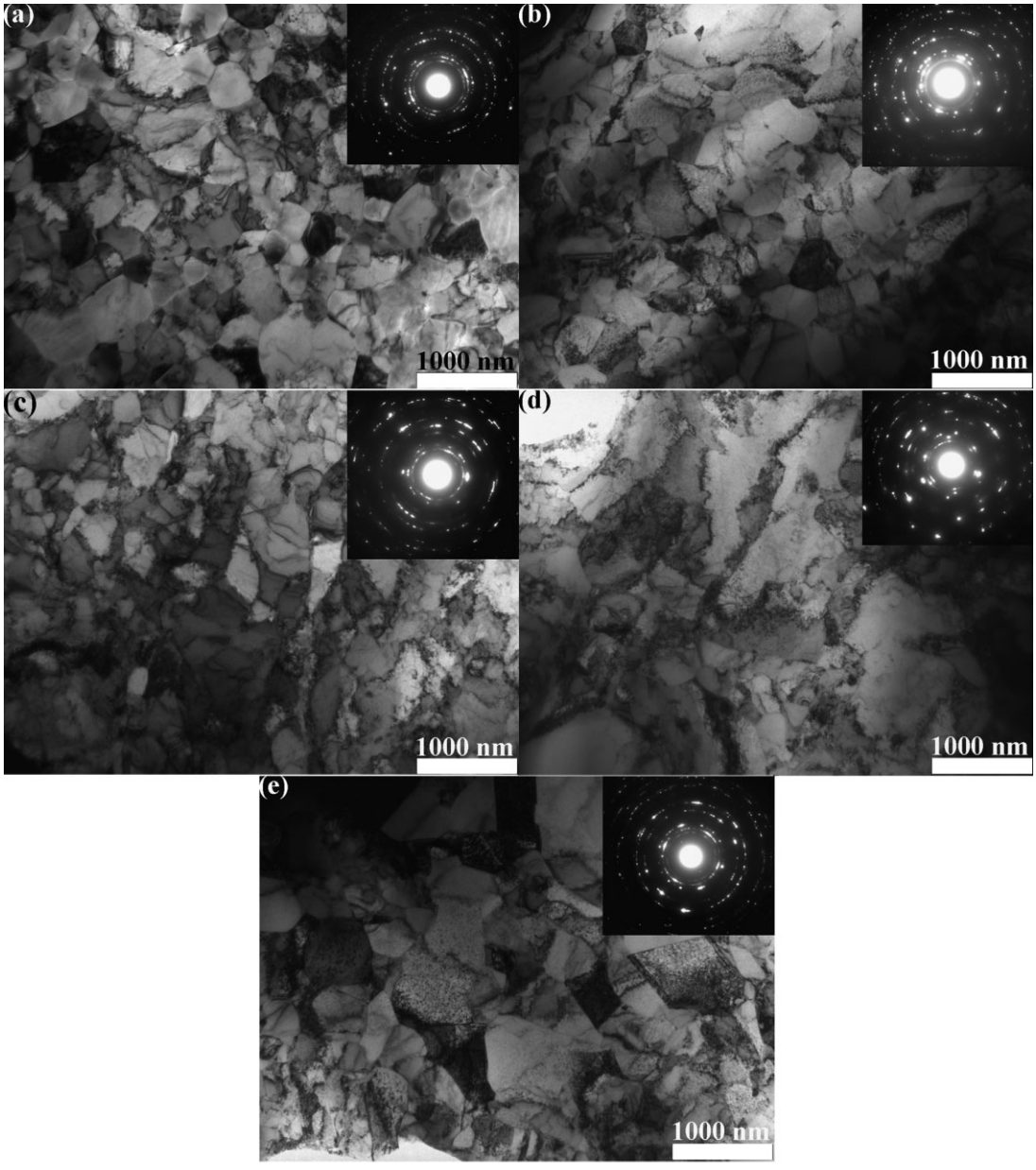

Fig. 1. TEM images and corresponding SAED patterns (taken with the aperture size of ≈6 μm) of UFG Cu processed by ECAP at different temperatures: (a) RT; (b) 373 K; (c) 423 K; (d) 473 K; (e) 523 K.

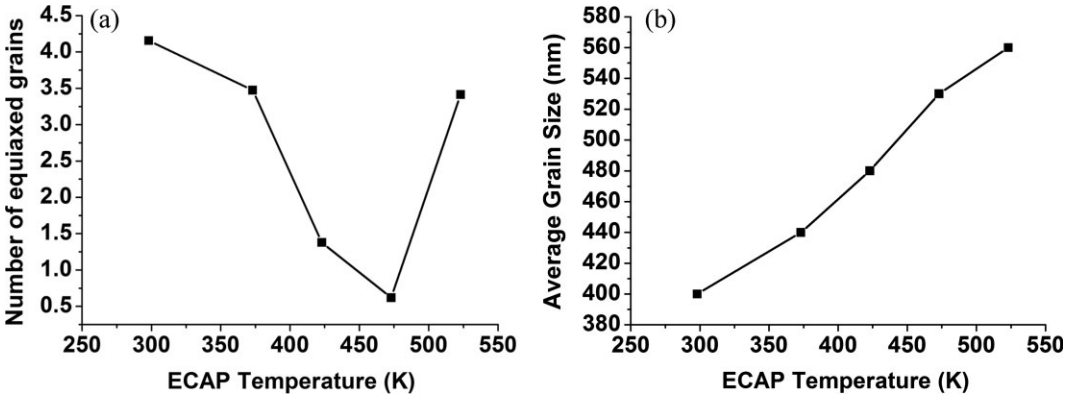

Fig. 2. (a) Average number of equiaxed grains per 10 μm² and (b) average grain size of the equiaxed grains in the UFG Cu samples processed by ECAP at different temperatures.

together with the corresponding SAED patterns taken with an aperture of ≈6 μm in diameter. A homogeneous microstructure, which primarily consisted of equiaxed grains, developed in the sample processed at RT [Figure 1(a)]. The average grain size was ≈400 nm. The reports available in the literature indicate that average grain/subgrain sizes ranging from ≈200 to 400 nm were obtained by RT ECAP of Cu.[27–34] The measured relatively large average grain sizes in this work may be due to the characteristics of the statistical measurements in which low-angle subgrain boundaries were disregarded whereas measurements in some other studies recorded the smallest grain-subdividing elements. The SAED pattern of the RT EACP Cu sample shown in Figure 1(a) consists of continuous rings which indicate a high fraction of high-angle grain boundaries.

The microstructure of the sample processed at 373 K, as shown in Figure 1(b), was similar to that of the sample processed at RT, with equiaxed grains and high-angle grain boundaries prevailing. However, a low percentage of dislocation cell structures was also present in the microstructure. The average grain size of the sample of ≈440 nm was also slightly larger. Nevertheless, the microstructure after ECAP at 423 K [Figure 1(c)] was significantly different, as dislocation cell structures overwhelmed the equiaxed grains, and the coexistence of the two elements indicated the inhomogeneous nature of the microstructure. The SAED pattern exhibited net morphology, indicating that primarily low-angle boundaries were present. The average grain size for this condition was ≈480 nm.

The microstructure of the sample processed at 473 K consisted primarily of dislocation cell structures [Figure 1(d)] and equiaxed grains were seldom present. The SAED pattern showed some discrete diffraction spots indicating a very low fraction of high-angle boundaries. The average grain size was ≈530 nm which was larger than that after pressing at 423 K. From the TEM images, the dislocation cell size was also larger than that at 423 K although it was not quantitatively measured. During the statistical grain size analyses, 80 TEM images with a magnification 63 000 (the area of each image was 14.5 μm²) were used for each sample and the grain size measurements were conducted on grains with well-defined grain boundaries: these grains were nearly equiaxed and were on or near a major zone axis. The numbers of equiaxed grains counted were 482, 403, 160, and 72 in the RT, 373, 423, and 473 K processed samples, respectively. The average number of equiaxed grains per 10 μm² in each sample was calculated and it is shown in Figure 2(a). Therefore, as the ECAP temperature increased, the fraction of equiaxed grains decreased as compared to that of the dislocation cell structures, which was another indication that the fraction of high-angle boundaries dropped, as equiaxed grains counted in this study tended to have high-angle grain boundaries. This trend is also consistent with the results obtained from the SAED patterns.

The observation that increasing ECAP temperature leads to a decrease in the fraction of high-angle grain boundaries and an increase in the grain size, as shown in Figure 2, are in agreement with reports on ECAP of Al and Al alloys at elevated temperatures.[10–13,20–25] A mechanism was proposed for the decrease of boundary misorientations formed at elevated temperatures,[10] which was supported by later studies.[11,21] The transformation of low angle boundaries into high angle boundaries is realized through the impingement and absorption of moving dislocations into the boundaries during deformation. At higher pressing temperatures, the rate of recovery increases and it is easier for dislocations to be annihilated within the (sub)grain interiors by climb or cross slip rather than being absorbed in the boundaries. Consequently, the evolution of the microstructure into an array of high-angle boundaries is less efficient at elevated temperatures, thereby favoring the retention of the low-angle boundaries.

The major difference between elevated temperature ECAP of Cu in this study and that of Al and Al alloys in the literature lies in the large or even dominant portion of the dislocation cell structures that exists in the Cu samples after ECAP (except after processing at 373 K) while a microstructure consisting of equiaxed grains with very few dislocation cell structures was achieved in most Al and Al alloys after ECAP[10–13,20–24] (except only when the ECAP temperature for 2219 Al alloy

ADVANCED ENGINEERING MATERIALS

was as high as 748 K and there was an inhomogeneous microstructure composed of comparable fractions of equiaxed grains and dislocation cell structures[25]). The microstructure evolution during SPD including ECAP starts with the subdivision of grains into dislocation cells which are formed through deformation-induced dislocation accumulation and recombination.[40–42] As deformation proceeds, the dislocation cell boundaries are transformed into low-angle subgrain boundaries. The misorientations across subgrain boundaries increase with increasing strain, leading to the formation of high-angle grain boundaries.[42,43] This series of strain-induced processes are sometimes referred to as continuous dynamic recrystallization (CDRX), which involves the formation of arrays of deformation-induced low-angle boundaries (dislocation cell or subgrain boundaries) followed by their gradual transformation into high-angle grain boundaries upon further straining.[12,13,24,25,44,45] An increase in the deformation temperature and a concomitant rise in the recovery rate slow down the CDRX kinetics and microstructure development. In addition, the microstructure evolution in Cu during ECAP is significantly slower than that in Al and at the same imposed strain the fraction of low-angle boundaries in Cu is always higher than that in Al.[27,46] Consequently, in the case of elevated temperature ECAP of Cu in this study, a large fraction of dislocation cell structures are retained in the microstructure, especially at the higher temperatures of 423 and 473 K, while an equiaxed grain structure with high-angle or low-angle grain/subgrain boundaries is attained in the microstructure of Al and Al alloys after ECAP at elevated temperatures. However, it may be anticipated that, with an increase in the number of ECAP passes and therefore a higher strain so that the microstructure evolution processes are more complete, a homogeneous microstructure consisting primarily of equiaxed grains separated by high-angle grain boundaries may be achieved for Cu after ECAP at elevated temperatures. This suggestion is supported by a report that the fraction of high-angle grain boundaries was as high as 75% in a 7475 Al alloy after ECAP at 673 K to a high strain of 12 whereas the fraction was only ≈10% with an imposed strain of 3.[21]

2.2 Microstructure after ECAP at 523 K

The microstructure obtained after ECAP at 523 K [Figure 1(e)] appears to contradict the mechanism described earlier that the fraction of equiaxed grains or high-angle grain boundaries decreases at elevated temperatures. From the TEM image, a large proportion of equiaxed grains is present in the microstructure with sharp grain boundaries and the SAED pattern exhibits continuous rings and is similar to the sample processed at 373 K thereby indicating a significant fraction of high-angle grain boundaries. In addition, the average number of equiaxed grains per $10\,\mu m^2$ in the sample increased drastically compared to that in the 473 K processed sample [see Figure 2 (a)]. A low fraction of dislocation cell structures was also present in the microstructure. The experimental results obtained for the sample processed at 523 K can not be explained on the basis of the mechanism described earlier for the samples processed at the other four temperatures, following which the microstructure should consist of a dominant fraction of dislocation cell structures and a very low proportion, if any, of equiaxed grains.

The microstructural features of the sample processed at 523 K warrant analysis and discussion. The ECAP of Al alloys at some relatively high temperatures has sometimes been reported to produce a dramatically larger average grain size than that obtained at lower elevated temperatures[11] or a bimodal grain size distribution.[13] These phenomena were ascribed to static annealing/recrystallization which may occur during ECAP passes by exposure of the as-deformed material in the hot ECAP channels and reheating between ECAP passes. The temperature for the onset of significant static recrystallization of Cu processed by ECAP at RT is reported as usually in the range of 423–483 K, depending on the processing parameters of ECAP and therefore the stored strain energy in the sample, as well as on the purity of the material.[26,27,47–49] The static recrystallization temperature of Cu processed by ECAP at elevated temperatures should be higher than that of the sample processed at RT because the stored strain energy in the former is lower than that in the latter due to the higher recovery rate at higher temperatures. In related work, it was reported that the static recrystallization temperature increased from 453 K for OFHC Cu (99.99%) processed by ECAP at RT to 507 K for Cu processed at 473 K.[26] It can be expected that the static recrystallization temperature is above 523 K for the Cu sample (99.9%) processed by ECAP at 523 K in this study. In addition, static annealing of SPD-processed Cu usually produces by static recrystallization a bimodal grain size distribution with the larger grain size on the order of several microns.[27,36,37] For the Cu sample processed at 523 K in this study, a bimodal grain size distribution was not found and the average grain size of ≈560 nm was only slightly larger than the value of ≈530 nm for the sample processed at 473 K. Therefore, static recrystallization is not operative.

The presence of a large fraction of equiaxed grains with sharp grain boundaries in the Cu sample processed at 523 K is attributed to discontinuous dynamic recrystallization (DDRX). In related work it was also proposed that DDRX occurred during ECAP of Cu at different temperatures but it was suggested that DDRX took place even at RT.[26] DDRX is the classical type of dynamic recrystallization and it operates in materials with relatively low stacking fault energies during hot deformation and involves the processes of nucleation and grain growth.[50] Formation of nuclei predominantly occurs at pre-existing grain boundaries through the local migration, i.e., bulging, of grain boundaries at sites of sufficient stored energy.[51] The recrystallization then proceeds through the growth of the new nucleated grains by migration of their grain boundaries, thereby leading to the consumption of the deformed matrix.[52,53] Hot plastic deformation with DDRX can cause significant grain refinement and is recognized as an important tool for controlling the properties of materials.[54,55]

The DDRX processes are known to be dependent on temperature, stress, strain, strain rate, and initial microstructure. Experimental studies of DDRX in Cu have been carried out primarily during hot compression with strain rates of $\approx 10^{-5}$–10^{-1} s^{-1} at temperatures of ≈473–1073 K.[54,56–59] In the present study, DDRX occurred during ECAP of Cu at 523 K, while CDRX took place during ECAP at temperatures ≤473 K. In the case of Al and Al alloys, which have high stacking fault energies and therefore high recovery rates, DDRX is usually completely inhibited[44,50] and only CDRX operates during hot deformation (including hot ECAP) at all temperatures.[12,13,24,25,44,45] During hot compression of a Ni-20% Cr alloy with low stacking fault energy, a change in mechanism of grain refinement from DDRX to CDRX was observed as the temperature decreased and the flow stress increased.[51] Decreasing the deformation temperature slows down the diffusion-controlled processes which inhibit the migration of grain boundaries over large distances and therefore leads to the suppression of DDRX at relatively low temperatures. Meanwhile, the recovery rate is low at relatively lower temperatures, which is a favorable condition for the evolution of strain-induced low-angle boundaries and the subsequent formation of high-angle grain boundaries. Therefore, CDRX is favored at lower temperatures. In addition, during ECAP at lower temperatures the pressing/flow stress is also higher which facilitates the operation of CDRX.

It should be noted that DDRX was not complete in the UFG Cu processed by ECAP at 523 K and there was a low fraction of dislocation cell structures. DDRX involves the competitive processes of dislocation generation by deformation and dislocation annihilation by recrystallization, generating inhomogeneous microstructure which consists of two structural components in the form of dynamic grains in various hardened stages and new recrystallized grains. A steady state, with the full development of equiaxed grains with a stable grain size, is achieved above a saturation strain at which a dynamic balance is reached between strain hardening and recrystallization.[53,60] The strain imposed during ECAP at 523 K is probably lower than the saturation strain. However, the equiaxed grains are better developed during ECAP at 523 K than at 473 K since the fraction of equiaxed grains for the former is much higher than for the latter (see Figure 2). The saturation strain required to reach a steady state for CDRX is generally much larger than for DDRX.[51,60] Remarkably larger strains are needed for the formation of strain-induced low-angle boundaries and the subsequent development of high-angle grain boundaries during CDRX.

2.3 Mechanical Behavior after ECAP

The ECAP temperature has a significant influence on the subsequent mechanical behavior of UFG Cu samples. Since two tensile tests were performed for each processing condition, representative engineering stress–strain curves may be presented for each condition as shown in Figure 3, while the mean values and the associated errors are summarized in Table 1. A general trend is that as the ECAP temperature increases so the strength decreases while the elongation/ductility is enhanced. The RT processed sample had a yield strength (0.2% offset strain) of 385 ± 5 MPa and an elongation to failure of 7.1 ± 0.4% and these values are similar to those reported in the literature.[29] Steady decreases in strength and increases in elongation were observed for the samples processed at 373 and 423 K while the sample processed at 473 K showed a significant increase in total elongation. Notably, the 523 K processed sample possessed a good combination of strength and ductility, with a yield strength of 215 ± 4 MPa and a total elongation of 33.2 ± 1.9%. It is noted that a coarse-grained Cu sample with an average grain size of 50 μm which was obtained by RT ECAP followed by annealing at 773 K for 2 h had a yield strength of 30 MPa and a total elongation of 65%.[61]

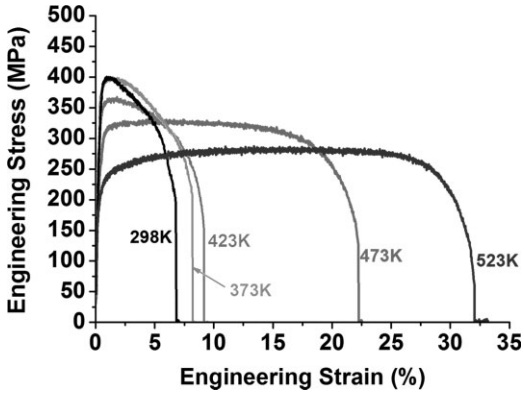

Fig. 3. Tensile stress–strain curves of UFG Cu samples processed by ECAP at different temperatures.

Table 1. Tensile properties of the UFG Cu samples processed by ECAP at different temperatures.

ECAP temperature [K]	Yield strength [MPa]	Ultimate tensile strength [MPa]	Uniform elongation [%]	Total elongation [%]
298	385 ± 5	400 ± 7	0.9 ± 0.1	7.1 ± 0.4
373	386 ± 10	400 ± 8	1.5 ± 0.4	8.4 ± 1.0
423	345 ± 3	368 ± 3	1.8 ± 0.3	9.5 ± 0.1
473	283 ± 6	331 ± 5	4.4 ± 0.6	22.6 ± 2.6
523	215 ± 4	287 ± 3	19.0 ± 1.0	33.2 ± 1.9

Compared to the total elongation, the uniform elongation before necking is generally a better measure of ductility since it is much less affected by the gauge length.[62] The uniform elongation is a direct indication of the strain-hardening rate. Figure 4 plots the yield strength and uniform elongation values achieved at different ECAP temperatures. Notably, the sample processed at 523 K exhibits a uniform elongation of 19.0 ± 1.0% which is a significant improvement over all other samples and represents an increase of more than three times compared with the sample processed at 473 K where the uniform elongation was 4.4 ± 0.6%. It should be noted that the yield strength of the 523 K sample only decreased by 24%

ADVANCED ENGINEERING MATERIALS

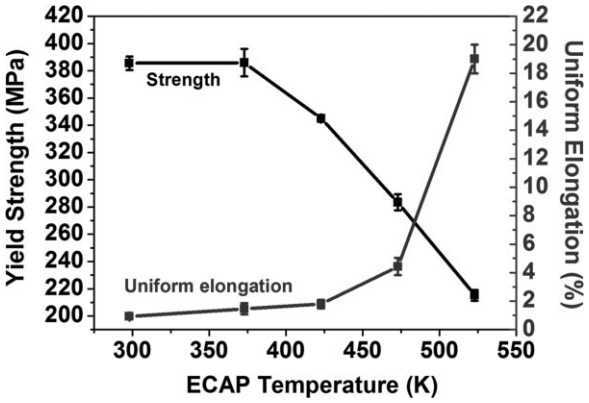

Fig. 4. Tensile yield strength and uniform elongation of UFG Cu samples processed by ECAP at different temperatures.

compared with that of the 473 K sample. The large uniform elongation of the 523 K sample indicates a significant strain-hardening rate during tensile testing which is partly attributed to the larger grain size and higher fraction of equiaxed grains. A larger grain size allows a greater capability for dislocation storage and accumulation and thus improves the strain hardening. A bimodal structure, in which micron-sized grains induce significant strain hardening, has been utilized as one of the major strategies to improve ductility.[36,63] In addition, the high fraction of equiaxed grains derived from DDRX probably has a low dislocation density which provides more space for dislocation accumulation during the tensile testing.

2.4 Dislocation Densities after ECAP

In order to further ascertain the reasons for the differences in mechanical behavior among samples processed at different temperatures, HRTEM was applied to study the dislocation densities of all five samples. During this investigation, HRTEM images of three grains were recorded for each sample. For the sample processed at RT, in which equiaxed grains dominate the microstructure, three equiaxed grains were studied; for the samples in which the fraction of equiaxed grains was higher than for the dislocation cell structures as in the 373 and 523 K samples, two equiaxed grains and one grain with a dislocation cell structure were studied; for the samples in which the fraction of dislocation cell structures was higher than for equiaxed grains as in the 423 and 473 K samples, one equiaxed grain and two grains with dislocation cell structures were investigated.

Figure 5 presents HRTEM images of the RT processed sample as an example to show the steps undertaken to obtain the dislocation density. Figure 5(a) shows a nearly equiaxed grain and its diffraction pattern on the [011] zone axis, Figure 5(b) depicts a representative lattice-fringe image, and Figure 5(c) presents the $(\bar{1}1\bar{1})$ planes obtained by inverse Fourier transformation of Figure 5(b) with seven dislocations marked by ''T'' at the dislocation cores. The dislocation density was determined by dividing the average number of dislocations per image by the area of an image. For the sample processed at RT, the dislocation density was $7.4/361\,\mathrm{nm}^2 = 2.05 \times 10^{16}\,\mathrm{m}^{-2}$. This value is in agreement with the dislocation density reported for UFG Cu processed by ECAP at RT.[47] The dislocation densities of all five processed samples and the associated errors are shown in Table 2. The general trend is that as the ECAP temperature is increased so the dislocation density decreases. Notably, there is a sharp drop in the dislocation density at 473 and 523 K which is in agreement with the conspicuous increase in the uniform elongation at these two temperatures (Figure 4). This indicates that the low dislocation density contributes to more space for dislocation accumulation.

The decrease in dislocation density at the ECAP temperature of 523 K is especially drastic. In addition, during the dislocation density investigation it was found that in the 523 K sample the average dislocation density in the two equiaxed grains $(1.2 \pm 0.3 \times 10^{14}\,\mathrm{m}^{-2})$ was one order of magnitude lower than the dislocation density in the grain with a

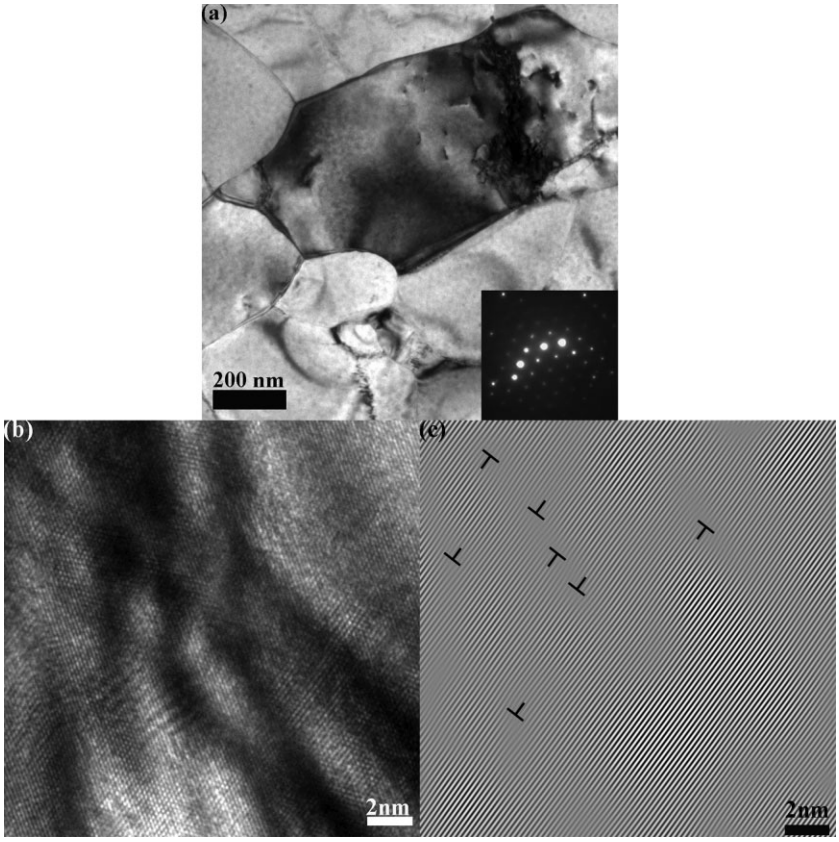

Fig. 5. (a) A nearly equiaxed grain in the Cu sample processed by ECAP at RT and its SAED pattern on the [011] zone axis; (b) a lattice-fringe image of the grain in (a); (c) the $(\bar{1}1\bar{1})$ crystallographic planes obtained by inverse Fourier transformation of (b), with dislocation marked by ''T'' at the dislocation cores.

Table 2. Dislocation density of the UFG Cu samples processed by ECAP at different temperatures.

ECAP temperature [K]	Dislocation density [m^{-2}]	Relative error [%]	Change in dislocation density between ECAP temperatures [m^{-2}]
298	$2.05 \pm 0.61 \times 10^{16}$	30	–
373	$1.82 \pm 0.43 \times 10^{16}$	23	-2.4×10^{15}
423	$1.70 \pm 0.48 \times 10^{16}$	28	-1.2×10^{15}
473	$1.12 \pm 0.35 \times 10^{16}$	31	-5.8×10^{15}
523	$6.9 \pm 5.7 \times 10^{14}$	83	-1.05×10^{16}

dislocation cell structure ($1.26 \pm 0.18 \times 10^{15}\,m^{-2}$). By contrast, in the other four samples, the dislocation density in the equiaxed grains was only slightly lower (within 50%) than in the grains with dislocation cell structures. Accordingly, the relative error associated with the dislocation density for the 523 K sample was 83% while for the other four samples it was within 30% (Table 2). This difference was related to the different grain refinement mechanisms operating at different ECAP temperatures, i.e., DDRX at 523 K and CDRX at the other temperatures. The observed difference between DDRX and CDRX in the dislocation densities is also in agreement with a report in which the variation with temperature of DRX mechanisms (DDRX and CDRX) was studied during hot-to-warm working of a Ni-20% Cr alloy.[51]

In DDRX, new grains nucleate and grow at the expense of the deformed matrix full of dislocations. Therefore, the microstructure consists of two structural components: dynamic grains in various hardened stages with relatively high densities of dislocations and new recrystallized grains relatively depleted of dislocations. The recrystallized grains are also deformed upon further straining and therefore are not free of dislocations. In contrast, during CDRX equiaxed grains with high angle boundaries are developed through the formation of deformation-induced low-angle boundaries followed by their transformation into high-angle grain boundaries upon further straining through the impingement and absorption of moving dislocations from the interiors into the boundaries. Therefore, the dislocation density in the equiaxed grains is only slightly lower than in the dislocation cell structures, which is supported by the report that during ECAP of Cu at RT the dislocation density at high strain (with equiaxed grains developed) is slightly lower than that at medium strain (with low-angle subgrain/dislocation cell boundaries dominant).[29,49] In the sample processed at 523 K, the equiaxed grains with very low dislocation density allow significant strain-hardening during the tensile test which leads to a large uniform elongation of the sample.

2.5 A Comparison with ECAP at RT Followed by Annealing

It is interesting to compare the mechanical behavior of UFG Cu obtained by ECAP at elevated temperatures with that of UFG Cu prepared by ECAP at RT and subsequent annealing. A bimodal structure with a mixture of micron-sized grains and UFG grains was obtained by ECAP of Cu at RT and annealing at 473 K for 40 min.[61] The volume fraction of micron-sized grains, which were produced by static recrystallization, was 65%.[61] The tensile yield strength and ultimate strength were 220 and 297 MPa, respectively, and the uniform elongation and elongation to failure were 18 and 34%, respectively.[61] The mechanical behavior was very similar to that of the sample processed by ECAP at 523 K in the present study. Therefore, it is suggested that ECAP processing at elevated temperatures may be an effective substitute for a combination of ECAP at RT and subsequent annealing at elevated temperatures.

3. Conclusions

ECAP of Cu was carried out at five different temperatures from RT to 523 K and the influence of temperature on microstructure evolution and mechanical behavior was studied by TEM, HRTEM, and tensile tests. The results show that:

(i) As the ECAP temperature is increased, the grain size increases, the dislocation density decreases, the strength decreases and the ductility is enhanced.

(ii) At ECAP temperatures from RT to 473 K, microstructural refinement occurs in accordance with CDRX which involved the formation of arrays of deformation-induced low-angle boundaries followed by their gradual transformation into high-angle grain boundaries upon further straining. The kinetics of grain refinement by CDRX are inhibited by an increase in the ECAP temperature which leads to a decreased ratio of equiaxed grains/high-angle grain boundaries to dislocation cell structures at higher ECAP temperatures.

(iii) DDRX, which includes the processes of nucleation and grain growth, is the mechanism responsible for grain refinement during ECAP at 523 K, inducing a high fraction of equiaxed grains with a very low dislocation density and therefore a high strain-hardening rate and ductility.

(iv) The sample processed at 523 K possessed a good combination of strength and ductility, suggesting that ECAP at elevated temperatures represents an alternative procedure to processing by ECAP at RT and subsequent annealing at elevated temperatures.

Received: March 8, 2011
Final Version: August 30, 2011
Published online: October 13, 2011

[1] R. Z. Valiev, T. G. Langdon, *Prog. Mater. Sci.* **2006**, *51*, 881.
[2] V. M. Segal, *Mater. Sci. Eng., A* **1995**, *197*, 157.
[3] Y. Iwahashi, Z. Horita, M. Nemoto, T. G. Langdon, *Acta Mater.* **1997**, *45*, 4733.

[4] Y. Iwahashi, Z. Horita, M. Nemoto, T. G. Langdon, *Acta Mater.* **1998**, *46*, 3317.
[5] V. V. Stolyarov, Y. T. Zhu, I. V. Alexandrov, T. C. Lowe, R. Z. Valiev, *Mater. Sci. Eng., A* **2001**, *299*, 59.
[6] K. Nakashima, Z. Horita, M. Nemoto, T. G. Langdon, *Acta Mater.* **1998**, *46*, 1589.
[7] R. B. Figueiredo, I. J. Beyerlein, A. P. Zhilyaev, T. G. Langdon, *Mater. Sci. Eng., A* **2010**, *527*, 1709.
[8] C. Xu, T. G. Langdon, *Scr. Mater.* **2003**, *48*, 1.
[9] P. B. Berbon, M. Furukawa, Z. Horita, M. Nemoto, T. G. Langdon, *Metall. Mater. Trans. A* **1999**, *30*, 1989.
[10] A. Yamashita, D. Yamaguchi, Z. Horita, T. G. Langdon, *Mater. Sci. Eng., A* **2000**, *287*, 100.
[11] Y. C. Chen, Y. Y. Huang, C. P. Chang, P. W. Kao, *Acta Mater.* **2003**, *51*, 2005.
[12] O. Sitdikov, T. Sakai, E. Avtokratova, R. Kaibyshev, Y. Kimura, K. Tsuzaki, *Mater. Sci. Eng., A* **2007**, *444*, 18.
[13] O. Sitdikov, T. Sakai, E. Avtokratova, R. Kaibyshev, K. Tsuzaki, Y. Watanabe, *Acta Mater.* **2008**, *56*, 821.
[14] D. H. Shin, J. J. Pak, Y. K. Kim, K. T. Park, Y. S. Kim, *Mater. Sci. Eng., A* **2002**, *325*, 31.
[15] I. Kim, J. Kim, D. H. Shin, C. S. Lee, S. K. Hwang, *Mater. Sci. Eng., A* **2003**, *342*, 302.
[16] Y. G. Ko, W. S. Jung, D. H. Shin, C. S. Lee, *Scr. Mater.* **2003**, *48*, 197.
[17] K. Xia, J. T. Wang, X. Wu, G. Chen, M. Gurvan, *Mater. Sci. Eng., A* **2005**, *410*, 324.
[18] C. X. Huang, G. Yang, Y. L. Gao, S. D. Wu, Z. F. Zhang, *Mater. Sci. Eng., A* **2008**, *485*, 643.
[19] E. J. Kwak, C. H. Bok, M. H. Seo, T. S. Kim, H. S. Kim, *Mater. Trans.* **2008**, *49*, 1006.
[20] U. Chakkingal, R. F. Thomson, *J. Mater. Process. Technol.* **2001**, *117*, 169.
[21] A. Goloborodko, O. Sitdikov, R. Kaibyshev, H. Miura, T. Sakai, *Mater. Sci. Eng., A* **2004**, *381*, 121.
[22] Y. Y. Wang, P. L. Sun, P. W. Kao, C. P. Chang, *Scr. Mater.* **2004**, *50*, 613.
[23] P. Malek, M. Cieslar, R. K. Islamgaliev, *J. Alloys Compd.* **2004**, *378*, 237.
[24] I. Mazurina, T. Sakai, H. Miura, O. Sitdikov, R. Kaibyshev, *Mater. Sci. Eng., A* **2008**, *473*, 297.
[25] I. Mazurina, T. Sakai, H. Miura, O. Sitdikov, R. Kaibyshev, *Mater. Sci. Eng., A* **2008**, *486*, 662.
[26] W. Huang, C. Y. Yu, P. W. Kao, C. P. Chang, *Mater. Sci. Eng., A* **2004**, *366*, 221.
[27] S. Komura, Z. Horita, M. Nemoto, T. G. Langdon, *J. Mater. Res.* **1999**, *14*, 4044.
[28] Y. M. Wang, E. Ma, *Acta Mater.* **2004**, *52*, 1699.
[29] F. Dalla Torre, R. Lapovok, J. Sandlin, P. F. Thomson, C. H. J. Davies, E. V. Pereloma, *Acta Mater.* **2004**, *52*, 4819.
[30] O. V. Gendelman, M. Shapiro, Y. Estrin, R. J. Hellmig, S. Lekhtmakher, *Mater. Sci. Eng., A* **2006**, *434*, 88.
[31] Q. Xue, I. J. Beyerlein, D. J. Alexander, G. T. Gray, *Acta Mater.* **2007**, *55*, 655.
[32] F. H. Dalla Torre, A. A. Gazder, C. F. Gu, C. H. J. Davies, E. V. Pereloma, *Metall. Mater. Trans. A* **2007**, *38*, 1080.
[33] S. V. Dobatkin, J. A. Szpunar, A. P. Zhilyaev, J. Y. Cho, A. A. Kuznetsov, *Mater. Sci. Eng., A* **2007**, *462*, 132.
[34] N. Lugo, N. Llorca, J. M. Cabrera, Z. Horita, *Mater. Sci. Eng., A* **2008**, *477*, 366.
[35] Y. H. Zhao, Y. T. Zhu, E. J. Lavernia, *Adv. Eng. Mater.* **2010**, *12*, 769.
[36] Y. M. Wang, M. W. Chen, F. H. Zhou, E. Ma, *Nature* **2002**, *419*, 912.
[37] Y. S. Li, Y. Zhang, N. R. Tao, K. Lu, *Scr. Mater.* **2008**, *59*, 475.
[38] Y. Iwahashi, J. T. Wang, Z. Horita, M. Nemoto, T. G. Langdon, *Scr. Mater.* **1996**, *35*, 143.
[39] M. Furukawa, Y. Iwahashi, Z. Horita, M. Nemoto, T. G. Langdon, *Mater. Sci. Eng., A* **1998**, *257*, 328.
[40] D. A. Hughes, N. Hansen, *Acta Mater.* **1997**, *45*, 3871.
[41] D. B. Witkin, E. J. Lavernia, *Prog. Mater. Sci.* **2006**, *51*, 1.
[42] M. Kawasaki, Z. Horita, T. G. Langdon, *Mater. Sci. Eng., A* **2009**, *524*, 143.
[43] V. M. Segal, *Mater. Sci. Eng., A* **1999**, *271*, 322.
[44] S. Gourdet, F. Montheillet, *Mater. Sci. Eng., A* **2000**, *283*, 274.
[45] T. Sakai, H. Miura, A. Goloborodko, O. Sitdikov, *Acta Mater.* **2009**, *57*, 153.
[46] O. V. Mishin, D. J. Jensen, N. Hansen, *Mater. Sci. Eng., A* **2003**, *342*, 320.
[47] X. Molodova, G. Gottstein, M. Winning, R. J. Hellmig, *Mater. Sci. Eng., A* **2007**, *460*, 204.
[48] Y. Zhang, J. T. Wang, C. Cheng, J. Q. Liu, *J. Mater. Sci.* **2008**, *43*, 7326.
[49] N. Lugo, N. Llorca, J. J. Sunol, J. M. Cabrera, *J. Mater. Sci.* **2010**, *45*, 2264.
[50] H. J. McQueen, *Mater. Sci. Eng., A* **2004**, *387*, 203.
[51] N. Dudova, A. Belyakov, T. Sakai, R. Kaibyshev, *Acta Mater.* **2010**, *58*, 3624.
[52] D. G. Cram, H. S. Zurob, Y. J. M. Brechet, C. R. Hutchinson, *Acta Mater.* **2009**, *57*, 5218.
[53] H. Hallberg, M. Wallin, M. Ristinmaa, *Comp. Mater. Sci.* **2010**, *49*, 25.
[54] A. Belyakov, H. Miura, T. Sakai, *ISIJ Int.* **1998**, *38*, 595.
[55] I. Salvatori, T. Inoue, K. Nagai, *ISIJ Int.* **2002**, *42*, 744.
[56] W. Gao, A. Belyakov, H. Miura, T. Sakai, *Mater. Sci. Eng., A* **1999**, *265*, 233.
[57] A. Manonukul, F. P. E. Dunne, *Acta Mater.* **1999**, *47*, 4339.
[58] A. M. Wusatowska-Sarnek, H. Miura, T. Sakai, *Mater. Sci. Eng., A* **2002**, *323*, 177.

[59] H. Miura, T. Sakai, S. Andiarwanto, J. J. Ionas, *Philos. Mag.* **2005**, *85*, 2653.
[60] F. Montheillet, O. Lurdos, G. Damamme, *Acta Mater.* **2009**, *57*, 1602.
[61] Y. H. Zhao, T. Topping, Y. Li, E. J. Lavernia, *Adv. Eng. Mater.* **2011**, in press.
[62] Y. H. Zhao, Y. Z. Guo, Q. Wei, T. D. Topping, A. M. Dangelewicz, Y. T. Zhu, T. G. Langdon, E. J. Lavernia, *Mater. Sci. Eng., A* **2009**, *525*, 68.
[63] Y. H. Zhao, T. Topping, J. F. Bingert, J. J. Thornton, A. M. Dangelewicz, Y. Li, W. Liu, Y. T. Zhu, Y. Z. Zhou, E. J. Lavernia, *Adv. Mater.* **2008**, *20*, 3028.

